Cumhuriyet Üniversitesi Fen Fakültesi
Fen Bilimleri Dergisi (CFD), Cilt:36, No: 3 Özel Sayı (2015)
ISSN: 1300-1949

Cumhuriyet University Faculty of Science
Science Journal (CSJ), Vol. 36, No: 3 Special Issue (2015)
ISSN: 1300-1949

A Study on the Effect of Implementing Waterproof Membrane on Reduction of Water Seepage from Earthen Dams (Case Study: Shahid Madani Earthen Dam, Tabriz, Iran)

Ali JAVDANİ[1], Dr. Mikael YUSEFZADEH-FARD[2], Dr. Gholam MORADİ[3]

[1]*Ms.c Geotechnical Engineering, Tabriz University, Tabriz, iran*

[2]*Ph.d Geotechnical Engineering, Academic member of Tabriz Azad University*

[3]*Ph.d Geotechnical Engineering, Academic member of Tabriz University*

Received: 01.02.2015; Accepted: 05.05.2015

Abstract. It is a major concern in engineering to evaluate the seepage rate for controlling earthen dams. With regard to the ever-increasing construction of earthen dams in Iran, it seems inevitable to make accurate assessments of the stability and leakage of water in order to achieve optimal operation and prevent possible problems. The seepage analysis in designing a dam is important in terms of stability and safety. Because the flow of water in the dam body and under the foundation causes pore pressure and seepage force to exceed allowable limits, where the stability of the dam body and foundation materials will face several problems such as piping and internal erosion of backfill and foundation materials, which will eventually lead to the destruction of the dam. Several engineering methods have been developed for precisely analyzing the seepage rate and estimating the output rate and pore water pressures generated at any part of the dam body and foundation, one of which is the most widely used numerical method known as "finite elements". In order to investigate the leakage of water from the dam and stability of its slope, the Shahid Madani Dam in Tabriz was selected as case study. This dam is located five kilometers from the city of Tabriz, East Azerbaijan Province, Iran. The specifications of the dam were inserted as input date into software Seep/W and Slope/W, which are the basis for Seep/W numerical finite element method and the basis for Slope/w limit equilibrium method. The results showed that the rate of seepage in the earthen dam fall within the allowable limit. Moreover, the stability of embankments fulfills the factor of safety with regard to the type of material used.

Keywords: seepage, earthen dam, finite elements, Seep/w, Slope/w

1. INTRODUCTION

Iran stretches 1,648,195 square kilometers across southwest Asia. The climate is arid and semiarid as compared to other regions around the world. The average annual precipitation is about 250 mm, less than average rainfall in Asia and about a third of the global average. Roughly 80 percent of the annual precipitation occurs during 3 months.

The uneven spatial and temporal distribution of precipitation and surface currents compatible with water and severe changes between years are the hydrological characteristics of a large part of Iran. Therefore, the Persians of old times always need to take steps to maintain and regulate water use so as to attain the availability of water for drinking, agriculture and power generation. Hence, the dam development has long been concerned in Iran. The oldest dam once built in the country is called Kebar near Qom. Another ancient dam in the country is Korit in Tabas. Iran, ranks third in dam construction right after Turkey and China [1]. The current number of dams in the operation phase is about 228 while the cases under construction amount to 94 projects. There are 216 dam construction projects under study [2].

Dam is a building that separates one part from the other, often used in the sense of a wall or structure that prevents water flow aimed at storage or deviation [3]. Dam construction serves the following:

---

*Corresponding author. *Email address*: *ali_javdani6464@yahoo.com*

Special Issue: The Second National Conference on Applied Research in Science and Technology

1. Irrigation
2. Drinking
3. Hydraulic power or energy generation
4. Flood Control
5 Aquaculture and Building a recreational space
6. Refreshing the regional air and yielding optimal impact on the environment [4].

Dams are mainly classified into two types, concrete and earthen. Concrete dams are generally used for narrow high valleys. As for wide valleys, it is very common to build earthen dams. Earthen dam is a structure composed of particles attached to soil or gravel, in various sizes, which is necessary to stand before the flow of water and store it. In this type of dams, the shear strength of the soil resists against the forces. Earthen dam are of three homogeneous, homogenous and gravel designs [4].

1.1. The scientific theory of seepage

Water is always flows from high energy to low energy levels. The energy of water at any point is proportional to the load of water in that point $\left(E \propto h\right)$

$$h_A = z_A + \frac{P_A}{\gamma_w} + \frac{V_A^2}{2g} \text{(Bernoulli equation)} \tag{1}$$

Pass rate of water in the soil is insignificant. $\left(V_A \ ; \ 0\right)$

$$h_A = z_A + \frac{P_A}{\gamma_w} = z_A + \frac{U_A}{\gamma_w} \text{(Bernoulli equation for soil mechanics)} \tag{2}$$

If water should flow from point A to point B, two points should be unequal in terms of load ($h_A > h_B$). In other words, the two points should be different in load values. The less distance between the two points, the faster water will pass.

$$V \propto \Delta h, V \propto \frac{1}{\Delta L} \tag{3}$$

$$V \propto \frac{\Delta h}{\Delta L} \rightarrow V \propto i \rightarrow V = k.i = k\frac{\Delta h}{\Delta L} = k\frac{h}{L} \tag{4}$$

The above equation is called the Darcy equation, indicating that the velocity of passing is proportionate to the water gradient (i) the ratio of which is called soil permeability.

Soil permeability (K) deals with fine and coarse grains of soil and poreness and emptiness of soil, sharp edges and rounded corners of the soil, water temperature and density

$$k = \frac{\gamma_w}{\eta}.\bar{k} \tag{5}$$

In the above equation, we have:

$\bar{k}$: Absolute permeability of the soil dependent on porosity and shape of aggregates

η: Dynamic viscosity of water

γ_w : Specific weight of water

K: Soil permeability coefficient

The basis required for analysis of leakage was developed by Darcy about 150 years ago. Darcy carried out experiments, the results of which led to the creation of Darcy's Law Darcy's law shows that the speed with which water seeps under pressure gradients through a microporous layer such as soil is directly correlated with the initial hydraulic gradient. Later in the 1880s, Forchheimer proved that the distribution of water pressure and water flow rate within a layer seeping water will follow the Laplace equation [7].

2. LITERATURE REVIEW

Hill (1993) conducted a study on leakage in hydraulic structures [8] located on a non-isotropic earthen foundation. He examined the issue for different combinations of non-isotropic materials, angle of main axis in elliptic hydraulic conductivity along the horizontal axis, length of floor, depth of crushed planes, and depth of the porous layer through the finite element method presented below:

1) The variations of maximum output gradient of the downstream outlet structures is independent from the degree at which construction materials are non-isotropic.
2) For all modes, when the soil bedding makes an angle (ɵ <90) with the horizontal axis, the output gradient distribution of the earth to find the distribution of the gradient is lower than that for isotropic earthen foundation, where the differences raise by Kmax/Kmin.
3) For all structures placed on the soil stratification with an angle greater than 90 degrees and less than 120 degrees to the horizontal axis, the gradient distribution outlet in the bed downstream is higher than the gradient for the isotropic mode, where the differences raise by Kmax/Kmin.
4) The piezometric head distribution under the structure foundation depends on the inclination angle (ɵ) relative to the horizontal axis and type of the structure.
5) For the hydraulic structures with a single plane crushed upstream, the piezometric head distribution behaves in reverse in comparison with the piezometric head for structures with crushed plains downstream.

Using the finite element method, Khsaf (1998) studied the leakage flow so as to analysis the seepage from permeable soil under hydraulic structures equipped with flow control instruments [9]. The results showed that the best way to reduce the uplift pressure id to set a cut-off at the upstream and also a filter at a certain distance from the cut-off.

Irzooki (1998) examined the water leakage in Al-Quadisiya, a dam in Iraq [10]. The results showed that the main source of the leakage from tank could firstly be found in the foundation. Secondly, the disintegration of the plaster structures led to water seepage from the tank from underneath the injected cement membrane.

Dunbar and Sheahan (1999) studied the problem of leakage at embankment dam at a village called Hodges which leaked for over 30 years, and many of its restructuring measures were investigated [11]. He examined the series of events occurred at the dam from 1968 to 1993. In this paper, the two software SEEP and FastSeep were used for the finite element analysis of leakage. The results showed that there was a leak in the dam due to inaccurate assumptions about the soil profile of the dam foundations, walls, drainage and ancillary walls as well as insufficient subsurface information prior to design and construction phase.

Hosseini and Fard (2002) investigated the development of porous water pressure at the core of earthen dams during the simultaneous construction and operation [12]. The explanation was that the construction of large dams and embankments usually takes a long time. Thus, operation of the dam water while it is still under construction may be an effective way to benefit from certain advantages of the project before the construction is completed. The construction process leads to more pore water pressure, where operation leaves a similar impact on the dam core. This paper therefore examines the development of pore water pressure at the most critical point of an embankment dam due to the simultaneous operation and construction.

In another study, Yilmaz and Ersin (2004) examined the correct choice of materials for the dam core for Lower Cekerek Basin, Tokat, Turkey [13]. With regarding the fact that for impermeable materials, optimum moisture content, density, aggregate (Gs), liquid limit (L.L), plasticity index (Ip)) and the degree of maximum dry density have been advised as follow to serve in the clay core dam (Yilmaz and Karacan, 1996) (γ_d) (ω_{opt}) [Quoted by 13]

$(\gamma_{\text{dmax}} > 1.6 \text{ g/cm}^3)$ $(\omega_{\text{opt}} = \%15\text{-}20)$,
$(G_s > 2.60)$ (L. L=%40-50), $(I_p = \%14\text{-}20)$

Brunos and Lopez (2011) [16] conducted a study titled "Evaluation of Internal Erosion Caused by the Passage of Water through the Dam Body", where they reported that factors such as capability of soil erosion, water flow rate through the soil mass and geometry of structure are the main factors contributing to soil erosion caused by the passage of water. They suggested that in order to prevent the occurrence of damage due to soil erosion, the following rules must be met:

A) Using homogeneous materials during the construction process.
B) Using the transition zone between the coarse and fine materials.
C) Using filter and drainage for entire earthen facilities exposed to water damage in the foundation or near the impermeable core.

In 2013, Naseh and Ghafuri carried out a study on the seepage paths at the left abutment of the Bidvaz dam in North Khorasan, Iran [17]. The results demonstrated that the limestone in the left abutment of "Tirgan" type was due to inhibition by the cement grout causing the leakage. They recommended that a grout membrane be applied in order to seal leaks in parts where they are likely to seep.

Hosni et al. (2013) composed an article titled "Dam Slope Stability and Seepage Analysis using Numerical Methods (case study on Ilam dam)," finding out that leakage of water from the dam was 0.836 L/sec [18]. To do this, they used Seep/W. As for modeling in the software, there were four different pore sizes considered (coarse, medium, fine and unsaturated). The value obtained from the mean of this mode was defined as leakage throughout the dam.

Rajeeth (2011) examined the causes of breakage at this dam [19]. The results of this study indicated that the occurrence of a flood in 2010 loaded large amounts of water to inside the dam reservoir, thus exceeding the predicted limit, which ultimately silt transported by flood led to overflow and collapse of the dam. Interestingly, some repairs were done in 2003 due to observations of a leakage in the dam.

One of the most devastating consequences of dam seepage involves liquefaction, in which case, Robertson (2010) used in their study the cone penetration test for a wide range of soil types prone to liquefaction [20].

Tayfur et al. (2005) conducted a case study on a dam in Poland called Jeiziorsko through the finite element method in comparison with ANN used to estimate the leakage of the dam [21]. Their results showed that the neural network desirably estimated the finite element method, and even in some cases better in case of seepage and flow of water from the dam.

In 2013, a study similar to the one by Poorkarimi Kukaneh et al. [22] focused on Fileh Khase dam in Hamedan so as to examine how satisfactory the performance of the neural network was for estimation of the flow paths of the dam. The results indicated there was acceptable accuracy of this method for estimating the flow paths and the leakage from Fileh Khase dam.

It is worth noting that the study by Ersayin (2006) [23] in Izmir, Turkey, titled "Investigation of Seepage from Earthen Dam Body Using Artificial Neural Network" demonstrated that the ANN method was capable of identifying a pattern of water level in the upstream, downstream and is piezometers, which made possible hoe to predict the location of leaks in the earthen dam body. However, it is said that this method yields no clear relationship between input and output data, incapable of justification in cases where they have not been predefined.

Yusef al-Labban (2007) carried out a case study on Al-Adhaim dam, reporting that the clay core significantly reduced leakage rate and output gradient [7].

3. MATERIALS AND METHODS

The leakage analysis of earthen dams is done in order to obtain the amount of seepage through the dam body and foundation as well as to determine the level of water in the core and outline of the stream network [17]. In order to analyze the structure and foundation of the dam seepage at Madani dam (Venyar) in Tabriz, the finite element method was used through a computer program called SEEP/W packaged in Geostudio. The finite element method was developed in the mid 1960s and was employed in many engineering problems. Fluid flow through porous media is one of the engineering issues where the finite element method has been successfully applied. Today, this method is used on a variety of issues concerning water flow through porous media, groundwater flow, and water flow across free surface and the hydrodynamic problems. Prior to the finite elements method, the "finite differences" was the only method of numerical analysis applied in engineering problems. Unlike the finite differences, the finite element method yields more general formula applicable to any form of physical borders and any combination of non-isotropic and homogenous boundary conditions and moving boundaries, free surface, environment variables, two-phase flows, etc [7].

The Geostudio software package is a geotechnical application based on finite elements and numerical methods, through which stress-strain analysis, flow, seepage, slope stability, dynamic analysis, and also rapid decline conditions can be examined. In this version of the program, there is posibility to create a finite element mesh for the model by the software itself. The program is based on the input parameters (such as soil permeability) and entering the water level in the upstream and downstream, phreatic level inside the core and shell, potential lines and passing currents through the foundation and the amount of leakage from the body and foundation of the dam [39].

3.1. The stability analysis of the dam was done through SLOPE/W.

In the finite element method, the partial differential equation is first converted into an integral equation which includes only first order derivatives. Then, the integral is applied on the elements of the given environment in which it is divided numerically. In this method, the various elements can be used in terms of geometrical shape and the number of nodes. Generally, the triangular elements are used to analyze leakage in the dam. Obviously, in the case the quadrilateral elements are applied, the operations would yield higher precision.

3.2. Seepage analysis using the finite element method

The soil mass elements must be separated for the analysis of seepage through finite element method. Square shapes and triangular elements are used for two-dimensional problems. Figure 1 shows the cross-section of a dam which is separated by triangular elements. The hydraulic head at each nodal point is obtained by solving the equation of governing current and taking into account the boundary conditions [7].

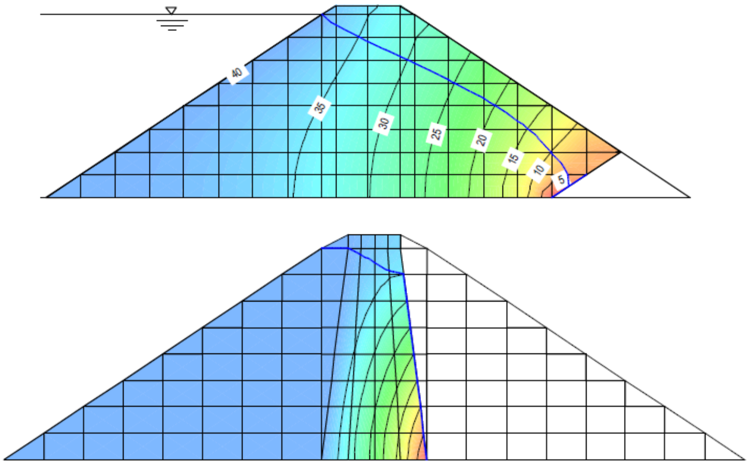

Figure 1. Element classification of dam section for finite element analysis [39].

Finite element formulation for steady-state leakage in two-dimensional mode using weighted residual method (Galerkin. 1986).

$$\int_A \begin{bmatrix} \frac{\delta}{\delta x}\{L\} \\ \frac{\delta}{\delta y}\{L\} \end{bmatrix} \begin{bmatrix} K_{wx} & 0 \\ 0 & K_{wy} \end{bmatrix} \begin{bmatrix} \frac{\delta}{\delta x}\{L\} \\ \frac{\delta}{\delta y}\{L\} \end{bmatrix} dA\{h_{wn}\} \int_s \{L\}^T V ds = 0 \qquad (6)$$

K_{wx}: Permeability in the x-direction
K_{wy}: Permeability in the y-direction

Rewriting equation 6 in a simplified form for the equation of governing currents, which leads to the following equation.

$$\int [B]^T [K_w][B] dA\{h_{wn}\} - \int_S [L]^T V_w ds = 0 \qquad (7)$$

[B]: Area derivative matrix formulated as follows:

$$\frac{1}{2A}\begin{bmatrix} (y_2 - y_3) & (y_3 - y_1) & (y_1 - y_2) \\ (x_3 - x_2) & (x_1 - x_3) & (x_2 - x_1) \end{bmatrix} \qquad (8)$$

Hydraulic head or flow rate must be specified at the boundary nodal points. The hydraulic heads specified in the boundary nodes are called Dirichlet boundary conditions. The specific flow rate crossing the border is represented by Neumann boundary condition. Newman is a term calculated in Equation 7 to determine the flow rate measured in the direction perpendicular to the boundary. For example, the specific flow rate V_w is converted in the direction perpendicular to a normal flow rate. The normal flow rate is converted into the nodal current Q_w. Q_{wi} and Q_{wj} respectively in the boundary nodes i and j represent a positive node where there is a penetration node or node acting as source. A negative current node represents evaporation in node where the node acts as a nozzle. When the flow rate is zero (permeable boundary), the second term in equation 7 is eliminated.

The finite element equation 7 can be written for each element in the equation and be assembled in the general current equation. This is done when the nodal compatibility is satisfied. Equation 7 is a nonlinear function, since the permeability is the function of matric suction, which is associated with the hydraulic head at nodal points.

$\{h_w\}$ represents the hydraulic heads for unknown variables in equation 7. Equation 7 is solved by an iterative procedure where for every replication the permeability of each element is a value depending on the matric suction at the three nodal points. The general flow equation is linear and can be solved simultaneously using Gauss elimination.

The calculated hydraulic heads at any nodal point are averaged again for determining the new permeability coefficient. K_w (u_a-u_w). The above steps are repeated until the permeability coefficients and hydraulic heads are not different more than a specified amount as compared to the results of the previous step. The hydraulic gradient along the x and y can be used to obtain the head element by deriving the hydraulic heads with respect to x and y.

$$\begin{Bmatrix} i_x \\ i_y \end{Bmatrix} = \left[B \right] \{h_{wn}\} \tag{9}$$

Where i_y and i_x: is: The hydraulic head gradient in the element are along x and y.

The hydraulic head gradient and flow rate at the nodal points are obtained by averaging yard values obtained from all elements surrounding the nodes. The weighted average is calculated in the average area of element.

In the finite element method, a given cross-section is divided into a number of triangular or quadrilateral elements that will influence the mesh procedure and the number of elements in the model results and whether convergence will be achieved. Usually, the dam body is meshed with triangular elements while the dam foundation is meshed with quadrilateral elements. The best mode for quadrilateral elements is when the angles are vertical. Furthermore, for quadrilateral elements, the interior angles are unacceptable equal to or greater than 180 degrees. In the selection of elements, the ratio of length to height affects the results. The results will be weaker with increasing length to height ratios. For long and narrow elements, the eight-node quadrilateral 9-point integration will be best suited to achieve convergence. As for the triangular elements, poorest mode is in extreme length and one point of integration. In general, the length-to-height ratio of 1 is best for achieving convergence. Nevertheless, as for long and narrow elements with length-height ratios of 5 or greater will yield poor results [7].

In this research, the finite element method for seepage analysis was used through Seep/W, the Geostudio module which is a geotechnical program based on finite elements and its main application is to analyze the water flow and leakage.

3.4. Research hypotheses

1- Given the conditions of the dam materials and foundation, the leakage is at the allowable limit.
2- The implementation of clay core will reduce leakage.
3- The implementation of waterproof membrane is effective in reduction of water leakage.

4. DISCUSSION AND CONCLUSIONS

4.1. Hypotheses formulated for analysis

1- With regard to its geometry at different levels, three periods of 21, 37 and 53 were respectively selected for analysis at positions including left abutment, bed and right abutment. The plan of the location for the selected dam sections at the right wing, bed and left wing have been illustrated in Figures (2), (3), (4) and (5). Section 37 is largest cross-section of the dam over the riverbed, where the height of the dam, thickness of alluvium and the height of the clay core have the maximum values. Sections (21) and (53) were considered with a distance of 80 meters from the middle section to be used for modeling through the body position and foundation at the left and right abutment over the river.

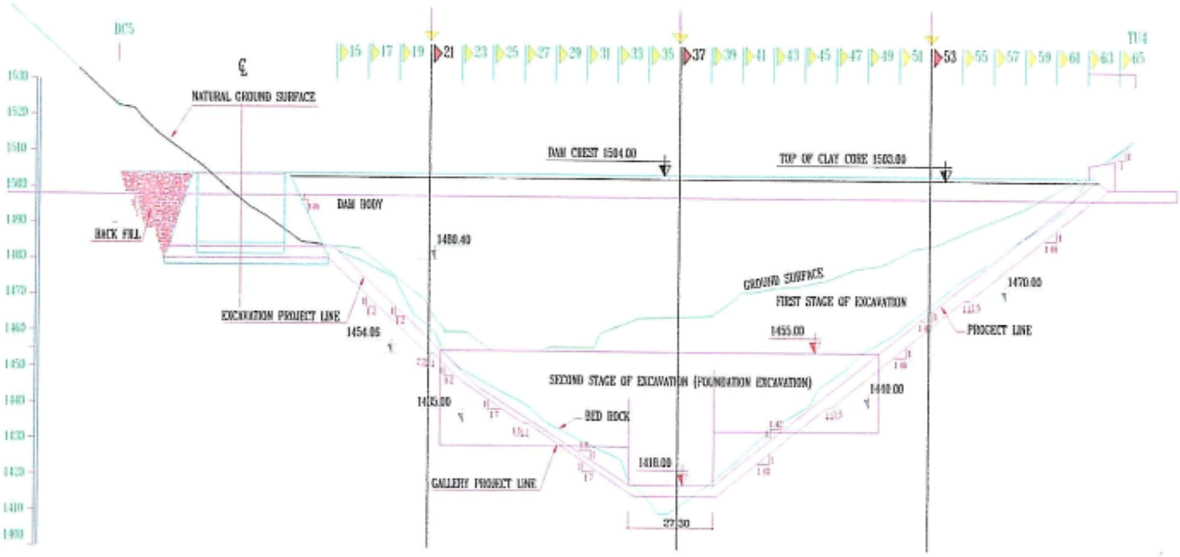

Figure 2. Location of the selected sections on the dam body

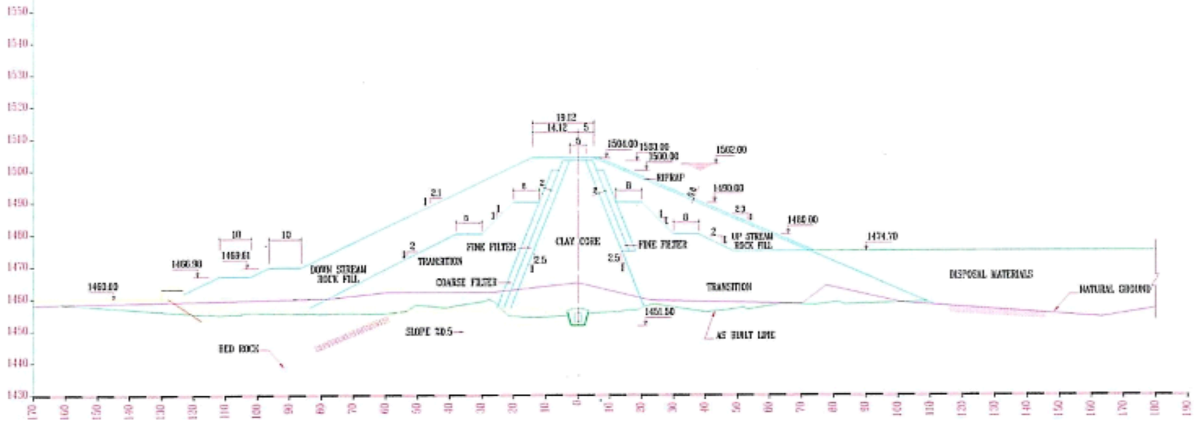

Figure 3. Cross-section of the dam and layers below foundation at the left abutment (section 21)

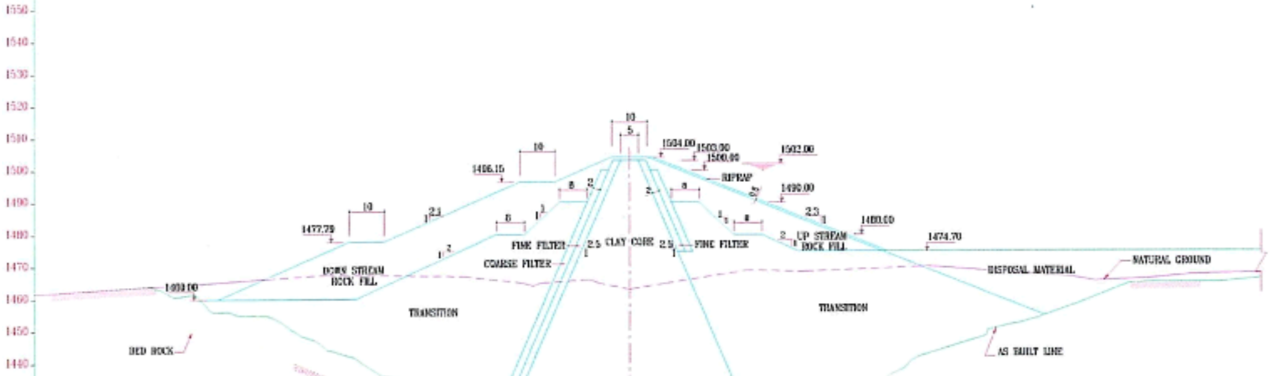

Figure 4. Cross-section of the dam and layers below foundation (section 37)

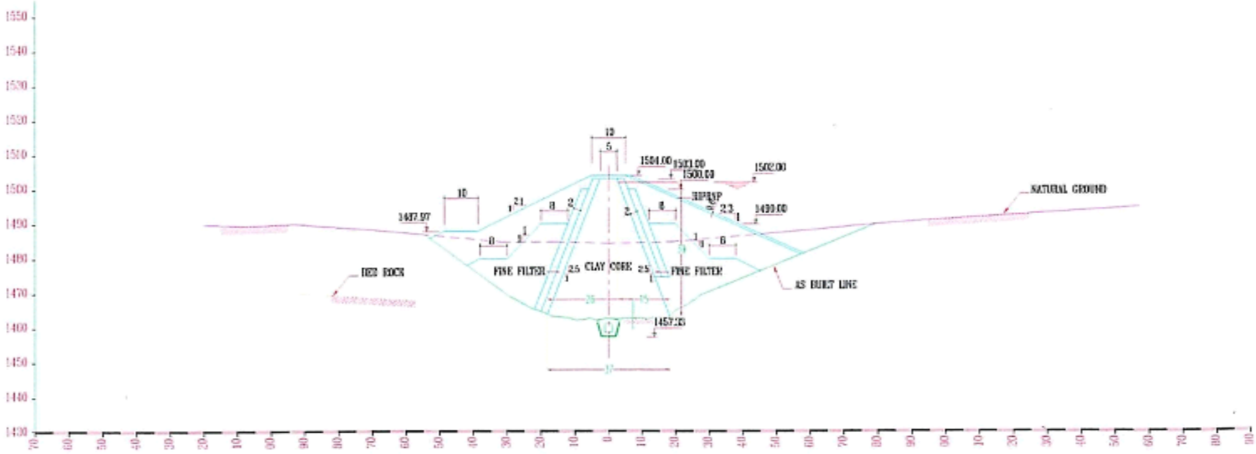

Figure 5. Cross-section of the dam layers below foundation at the right abutment (section 53)

4.2. Results of seepage analysis through Seep/W

In this study, based on the above information, several models for sections 21, 37 and 53 were developed by Seep/W on which leakage analysis was performed. Figures (6) to (11) demonstrate the result obtained by the analysis in the mentioned sections.

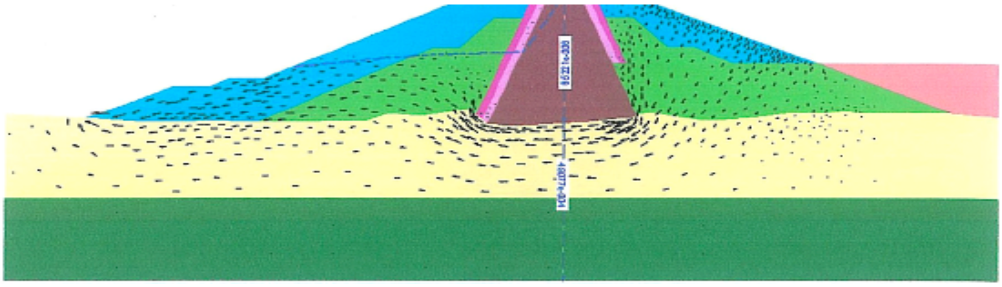

Figure 6. The result of the analysis of seepage without waterproof membrane (section 21)

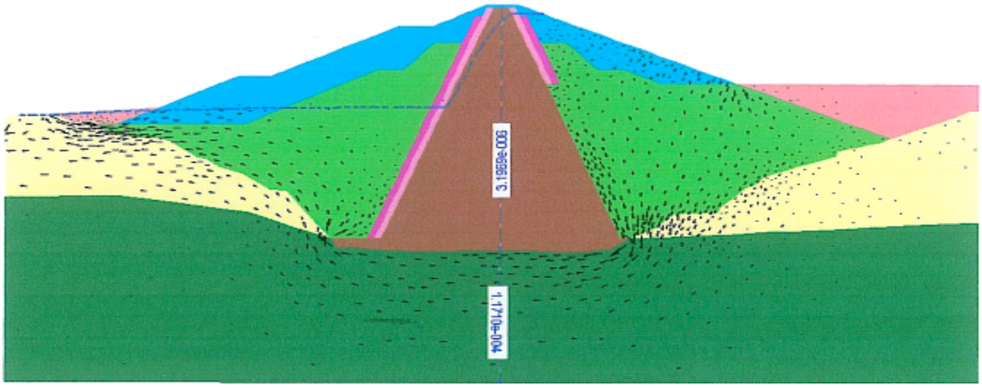

Figure 7. The result of the analysis of seepage without waterproof membrane (section 37)

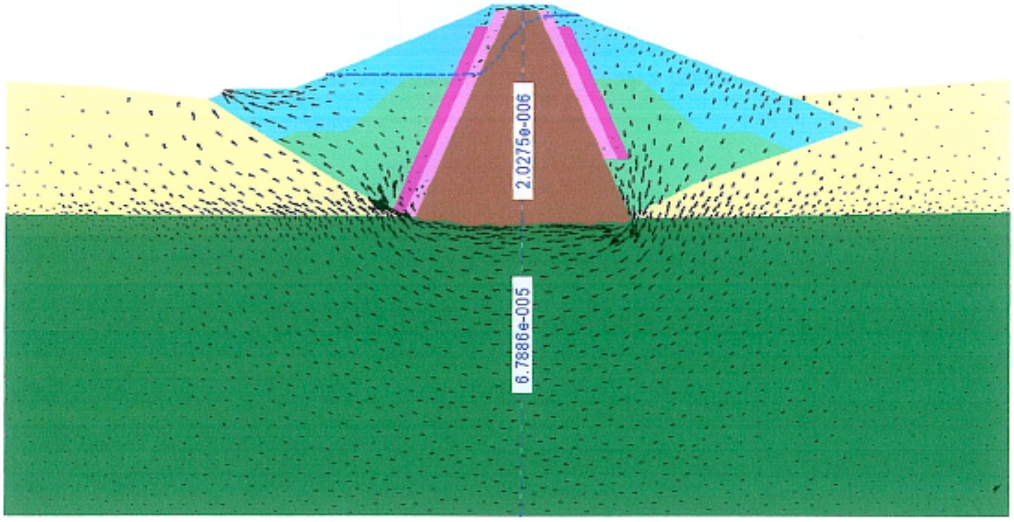

Figure 8. The result of the analysis of seepage without waterproof membrane (section 53)

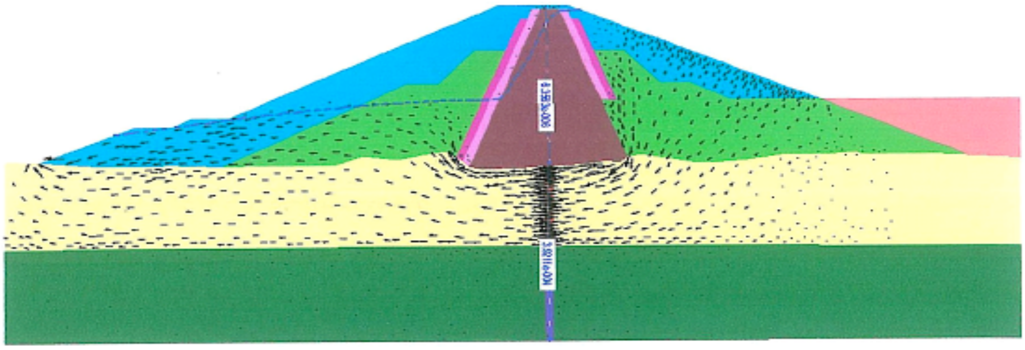

Figure 9. The result of the analysis of seepage with one row of waterproof membrane (section 21)

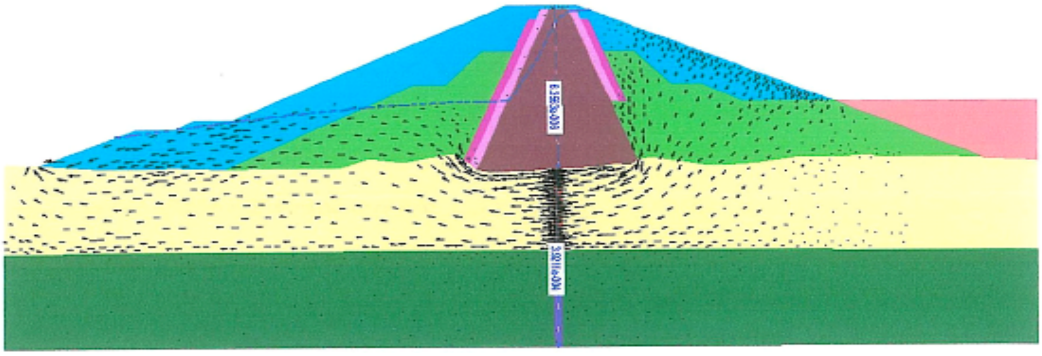

Figure 10. The result of the analysis of seepage with one row of waterproof membrane (section 37)

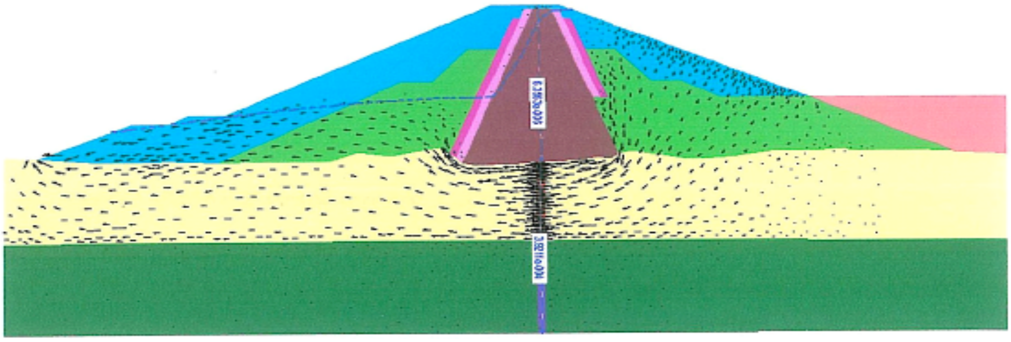

Figure 11. The result of the analysis of seepage with one row of waterproof membrane (section 53)

After the seepage analysis, the leakage rate was obtained for the given section as shown in Table (1).

Table 1. Analysis of seepage from body and foundation of the Shahid Madani Dam in Tabriz at given sections without waterproof membrane

Without waterproof membrane			
Total leakage $(m^3/s/m)$	Leakage from foundation $(m^3/s/m)$	Leakage from body $(m^3/s/m)$	Location
$^{4-}$10*87/4	$^{4-}$10*808/4	$^{6-}$10*523/6	Left abutment (section 21)
2.1*10^{4-}	$^{4-}$10*17/1	$^{6-}$10*197/3	Bed (section 37)
$^{5-}$10*99/6	$^{5-}$10*79/6	$^{6-}$10*028/2	Right abutment (section 53)

Table 2. Analysis of seepage from body and foundation of the Shahid Madani Dam in Tabriz at given sections with one row of waterproof membrane

One row of waterproof membrane			
Total leakage $(m^3/s/m)$	Leakage from foundation $(m^3/s/m)$	Leakage from body $(m^3/s/m)$	Location
$^{4-}$10*98/3	$^{4-}$10*921/3	$^{6-}$10*365/6	Left abutment (section 21)
$^{4-}$10*13/1	$^{4-}$10*102/1	$^{6-}$10*297/3	Bed (section 37)
$^{5-}$10*83/6	$^{5-}$10*642/6	$^{6-}$10*870/1	Right abutment (section 53)

Table 3. Analysis of seepage from body and foundation of the Shahid Madani Dam in Tabriz at given sections with two rows of waterproof membrane

Two rows of waterproof membrane			
Total leakage $(m^3/s/m)$	Leakage from foundation $(m^3/s/m)$	Leakage from body $(m^3/s/m)$	Location
$^{4-}$10*47/2	$^{4-}$10*432/2	$^{6-}$10*086/4	Left abutment (section 21)
$^{5-}$10*32/8	$^{5-}$10*950/7	$^{6-}$10*729/3	Bed (section 37)
$^{5-}$10*18/5	$^{5-}$10*957/4	$^{6-}$10*254/2	Right abutment (section 53)

Given the results of this section for the entire length of each section and the total amount of values, the amount of leakage was obtained according to tables (4) to (6).

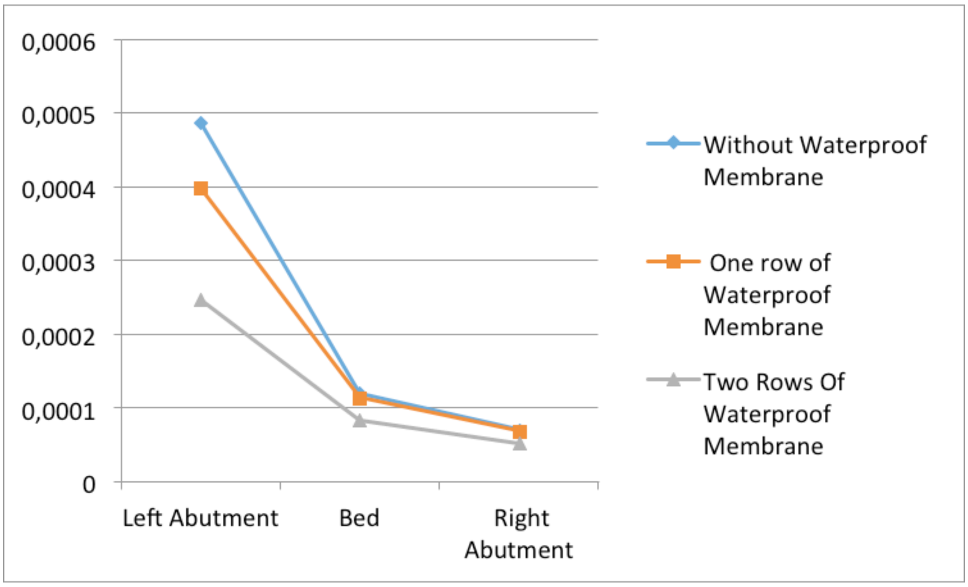

Figure 12. Analysis of seepage from body and foundation of the Shahid Madani Dam in Tabriz at given sections with various modes of waterproof membrane

Table 4. The amount of leakage obtained from the numerical analysis, without waterproof membrane at Shahid Madani Dam in Tabriz

Total leakage across the dam $\left(m^{۳}/s\right)$	Total leakage effective (m^3/s)	Effective length (m)	$\left(\overset{Q}{m^{۳}/s/m}\right)$	Location	
$^{4-}10*91/8$	$^{4-}10*89/4$	75	$6.523\text{x}10^{-6}$	Left abutment (section 21)	Dam body
	$^{4-}10*56/2$	80	$3.197\text{x}10^{-6}$	Middle (section 37)	
	$^{4-}10*46/1$	72	$2.028\text{x}10^{-6}$	Right abutment (section 53)	
$5/03\times10^{-2}$	$^{2-}10*61/3$	75	$^{4-}10*808/4$	Left abutment (section 21)	Foundation
	$^{3-}10*36/9$	80	$^{4-}10*17/1$	Middle (section 37)	
	$^{3-}10*89/4$	72	$6.790\text{x}10^{-5}$	Right abutment (section 53)	
$^{2-}10*12/5$	Total leakage from body and foundation without waterproof membrane				

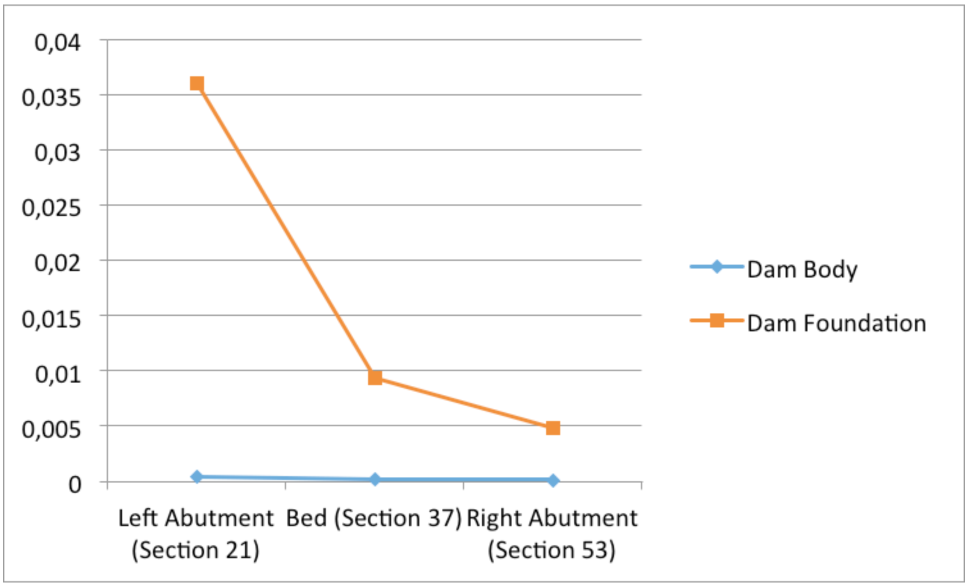

Figure 13. The leakage rate from dam body and foundation at Shahid Madani Dam in Tabriz at given sections without waterproof membrane

Table 5. Leakage rate obtained from numerical analysis with one row of waterproof membrane at Shahid Madani Dam in Tabriz

Total leakage across the dam $\left(m^{٣}/s\right)$	Total leakage effective (m^3/s)	Effective length (m)	$\overset{Q}{\left(m^{٣}/s/m\right)}$	Location	
$^{4-}10*76/8$	$^{4-}10*77/4$	75	$^{6-}10*356/6$	Left abutment (section 21)	Dam body
	$^{4-}10*64/2$	80	$^{6-}10*297/3$	Middle (Section 37)	
	$^{4-}10*35/1$	72	$^{6-}10*87/1$	Right abutment (section 53)	
$^{2-}10*3/4$	$^{2-}10*94/2$	75	$^{4-}10*921/3$	Left abutment (section 21)	Foundation
	$^{3-}10*82/8$	80	$^{4-}10*102/1$	Middle (Section 37)	
	$^{3-}10*78/4$	72	$^{5-}10*642/6$	Right abutment (section 53)	
$^{2-}10*39/4$	Total leakage from body and foundation with one row of waterproof membrane				

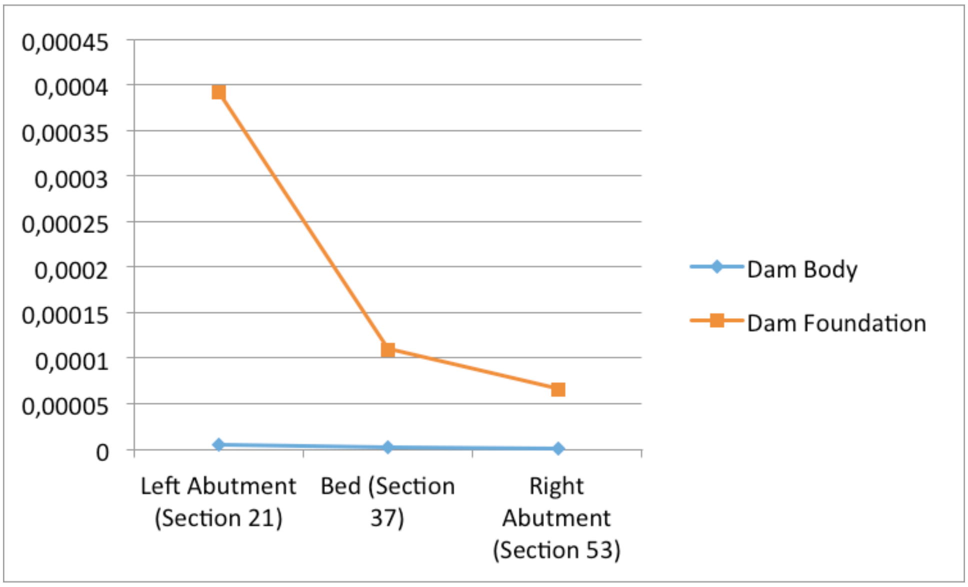

Figure 14. Leakage from the body and at the Dam Foundation Madani studied in a row grout curtain

Table 6. Leakage of numerical analysis, in two rows waterproof membrane barrier Shahid Madani

Total leakage across the dam $\left(m^3/s\right)$	Total leakage effective $\left(m^3/s\right)$	Effective length (m) (m)	$\overset{Q}{\left(m^3/s/m\right)}$	Location	
$^{4-}$10*67/7	$^{4-}$10*06/3	75	$^{6-}$10*086/4	Left abutment (section 21)	Dam body
	$^{4-}$10*98/2	80	$^{6-}$10*729/3	Middle (section 37)	
	$^{4-}$10*62/1	72	$^{6-}$10*254/2	Right abutment (section 53)	
2.82×10^{-2}	$^{2-}$10*82/1	75	$^{4-}$10*432/2	Left abutment (section 21)	Foundation
	$^{3-}$10*36/6	80	$^{5-}$10*95/7	Middle (section 37)	
	$^{3-}$10*57/3	72	$^{5-}$10*957/4	Right abutment (section 53)	
2.9×10^{-2}	Total leakage from body and foundation with two rows of waterproof membrane				

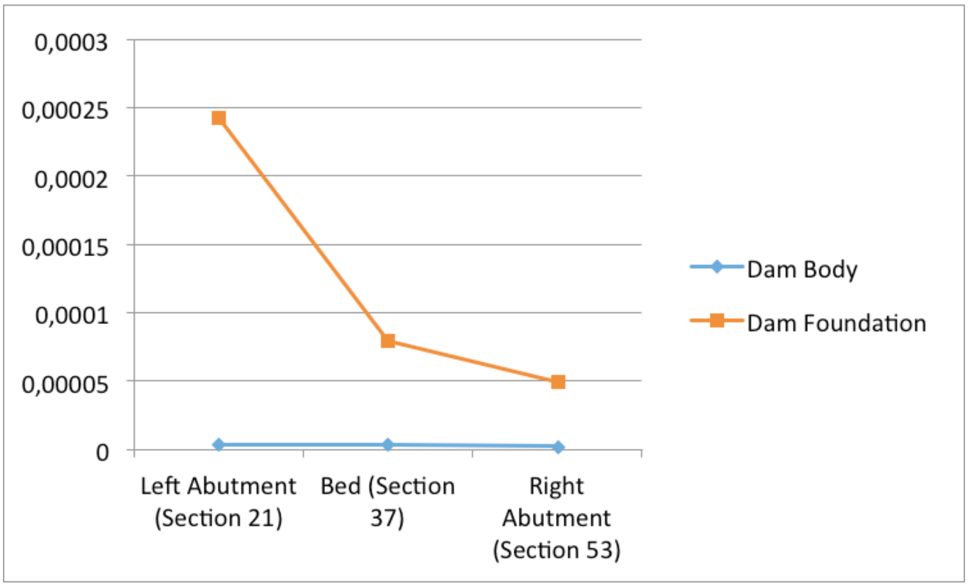

Figure 15. Analysis of seepage from body and foundation of the Shahid Madani Dam in Tabriz at given sections with two rows of waterproof membrane

To investigate the effect of the clay core on leakage reduction, re-analysis of the data concerning the Shahid Madani Dam was done assuming there was no clay core. The results in have been illustrated in Tables (7) to (12).

Table 7. Analysis of seepage from body and foundation of the Shahid Madani Dam in Tabriz at given sections without waterproof membrane, assuming there was no clay core

Without waterproof membrane			
Total leakage $(m^3/s/m)$	Leakage from foundation $(m^3/s/m)$	Leakage from body $(m^3/s/m)$	Location
$^{4-}$10*228/6	$^{4-}$10*144/6	$^{6-}$10*48/8	Left abutment (section 21)
$^{4-}$10*58/1	$^{4-}$10*54/1	$^{6-}$10*96/3	Bed (section 37)
$^{5-}$10*017/9	$^{5-}$10*759/8	$^{6-}$10*58/2	Right abutment (section 53)

Table 8. Analysis of seepage from body and foundation of the Shahid Madani Dam in Tabriz at given sections with one row of waterproof membrane, assuming there was no clay core

One row of waterproof membrane			
Total leakage $(m^3/s/m)$	Leakage from foundation $(m^3/s/m)$	Leakage from body $(m^3/s/m)$	Location
$^{4-}$10*943/4	$^{4-}$10*86/4	$^{6-}$10*389/8	Left abutment (section 21)
$^{4-}$10*503/1	$^{4-}$10*46/1	$^{6-}$10*38/4	Bed (section 37)
$^{5-}$10*735/8	$^{5-}$10*5/8	$^{6-}$10*35/2	Right abutment (section 53)

Table 9. Analysis of seepage from body and foundation of the Shahid Madani Dam in Tabriz at given sections with two rows of waterproof membrane, assuming there was no clay core

Two rows of waterproof membrane			
Total leakage (m^3/s)	Leakage from foundation $(m^3/s/m)$	Leakage from body $(m^3/s/m)$	**Location**
$^{4-}$10*282/3	$^{4-}$10*23/3	$^{6-}$10*23/5	Left abutment (section 21)
$^{4-}$10*057/1	$^{4-}$10*009/1	$^{6-}$10*847/4	Bed (section 37)
$^{5-}$10*68/6	$^{5-}$10*39/6	$^{6-}$10*9/2	Right abutment (section 53)

Table 10. The seepage rate obtained from numerical analysis of given sections at Shahid Madani dam without waterproof membrane, assuming there was no clay core

Total leakage across the dam (m^3/s)	Total leakage effective (m^3/s)	Effective length (m)	$\left(m^3/^{Q} s/m\right)$	Location	
11.3856*10^{-4}	$^{4-}$10*36/6	75	$^{6-}$10*48/8	Left abutment (section 21)	Dam body
	$^{4-}$10*168/3	80	$^{6-}$10*96/3	Middle (section 37)	
	$^{4-}$10*8574/1	72	$^{6-}$10*58/2	Right abutment (section 53)	
$^{2-}$10*43/6	$^{2-}$10*6/4	75	$^{4-}$10*144/6	Left abutment (section 21)	Foundation
	$^{2-}$10*2/1	80	$^{4-}$10*54/1	Middle (section 37)	
	$^{3-}$10*306/6	72	$^{5-}$10*57/8	Right	

				abutment (section 53)	
$^{2-}$10*54/6	Total leakage from dam without waterproof membrane				

Table 11. The seepage rate obtained from numerical analysis of given sections at Shahid Madani dam with one row of waterproof membrane, assuming there was no clay core

Total leakage across the dam (m^3/s)	Total leakage effective (m^3/s)	Effective length (m)	$\left(m^3/^{Q}s/m\right)$	Location	
$^{4-}$10*487/11	$^{4-}$10*291/6	75	$^{6-}$10*389/8	Left abutment (section 21)	Dam body
	$^{4-}$10*504/3	80	$^{6-}$10*38/4	Middle (section 37)	
	$^{4-}$10*692/1	72	$^{6-}$10*35/2	Right abutment (section 53)	
$^{2-}$10*425/5	$^{2-}$10*645/3	75	$^{4-}$10*86/4	Left abutment (section 21)	Foundation
	$^{2-}$10*168/1	80	$^{4-}$10*46/1	Middle (section 37)	
	$^{3-}$10*12/6	72	$^{5-}$10*5/8	Right abutment (section 53)	
$^{2-}$10*539/5	Total leakage from dam with one row of waterproof membrane				

Table 12. The seepage rate obtained from numerical analysis of given sections at Shahid Madani dam with two rows of waterproof membrane, assuming there was no clay core

Total leakage across the dam $\left(m^{۳}/s\right)$	Total leakage effective (m^3/s)	Effective length (m)	$\left(m^{۳}/^{Q}s/m\right)$	Location	
$^{4-}$10*887/9	$^{4-}$10*922/3	75	$^{6-}$10*23/5	Left abutment (section 21)	Dam body
	$^{4-}$10*877/3	80	$^{6-}$10*847/4	Middle (section 37)	
	$^{4-}$10*088/2	72	$^{6-}$10*9/2	Right abutment (section 53)	
$^{2-}$10*68/3	$^{2-}$10*42/2	75	$^{4-}$10*23/3	Left abutment (section 21)	Foundation
	$^{3-}$10*072/8	80	$^{4-}$10*009/1	Middle (section 37)	
	$^{3-}$10*6008/4	72	$^{5-}$10*39/6	Right abutment (section 53)	
$^{2-}$10*77/3	Total leakage from dam with two rows of waterproof membrane				

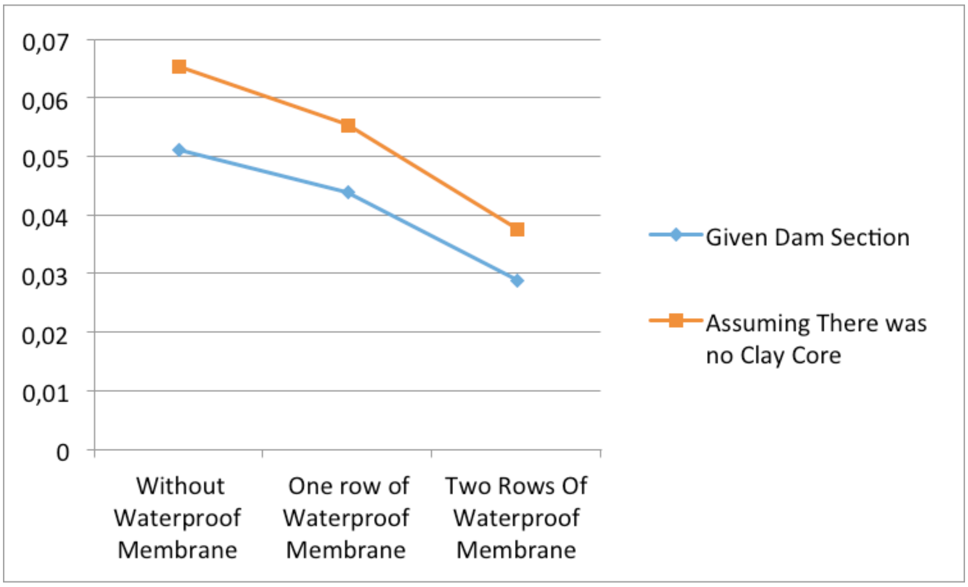

Figure 16. The seepage rate obtained from numerical analysis of given section at Shahid Madani dam with various modes of waterproof membrane, assuming there was no clay core

4.6. Stability analysis of Shahid Madani dam

The stability analysis of slopes at Shahid Madani dam using Slope/W modified through Bishop. In this method, the sliding surfaces are assumed to be a circular arc, and the balance of driving and resisting moments is evaluated. Finally, after analysis, the current materials were investigated to determine whether the safety requirements were met sufficiently. Then it was evaluated whether there was the possibility to change the material used, if necessary, so that it would not compromise safety measures. And potentially alternative materials applicable to the dam construction were introduced. In each sliding level, the factor of safety is equal to shear on stress resistance. Theoretically, the factor of safety less than one indicates a slippage whereas factor of safety greater than one indicates a non-slippage. According to USBR standards and other relevant literature available on controlling the stability analysis results, the minimum safety factor was introduced to the analyses as follow: [42].

1.5 for a steady leakage

1.3 at the end of construction

1.3 for the rapid depletion

Greater than 1.15 combined with the analysis of earthquake

The mechanical properties of materials in the foundation, shell and core at Shahid Madani dam used in the analysis of different conditions have been illustrated in Table 13.

Table 13. Mechanical properties of materials in foundation, shell and core of the Shahid Madani dam

Condition of analysis				parameter	Soil Material	Soil type No.
Earthquake condition	Rapid Draw-down	Steady Seepage	End of construction			
$19.23(KN/m^2)$				γ	Alluvium	1
$20.51(KN/m^2)$				γ_{sat}		
$20(kpa)$				C		
30				φ		
$19.2(KN/m^2)$				γ	Disposal	2
$19.6(KN/m^2)$				γ_{sat}		
0				C		
28				φ		
$22.5(KN/m^2)$				γ	Rock fill	3
$23(KN/m^2)$				γ_{sat}		
0				C		
48				φ		
$22.5(KN/m^2)$				γ	2Transition	4
$23(KN/m^2)$				γ_{sat}		
0				C		
42				φ		
$18(KN/m^2)$				γ	1Transition	5

$19(KN/m^2)$				γ_{sat}		
0				C		
38				φ		
$22.2(KN/m^2)$				γ	Core	6
$23.2(KN/m^2)$				γ_{sat}		
$15(kpa)$	$15(kpa)$	$7(kpa)$	$30(kpa)$	C		
23	23	30	20	φ		

4.6.1. The most critical section for stability analyses

The most critical section for stability analyses involves the section with the gretest elevation above the bedding rock. Considering the available maps, the deepest section was selected and the stability analysis was conducted on this section.

4.6.2 various positions of the analysis

The stability analyzes for the upstream and downstream slopes were carried out independently and in each case the factor of safety for critical cones was calculated as follows.
Various positions analyzed:

- end of construction and before operation
- Steady leakage conditions
- Rapid depletion of the tank
- Half full tank
- Earthquake

4.6.3. Results of analysis

All the analyses in different situations were done through SLOPE/W. Since the earthquake involves a more critical condition, the results conditions have been offered below:

4.6.3.1. Results of analyzes in the condition where the shell materials contain $\phi = 48$

4.6.3.1.1. End of construction and before operation and during earthquake

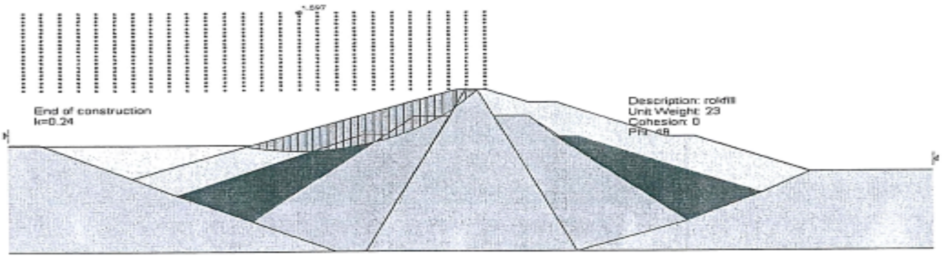

Figure 17. Upstream slope slippage at the end of construction and before operation 597/1=S_f

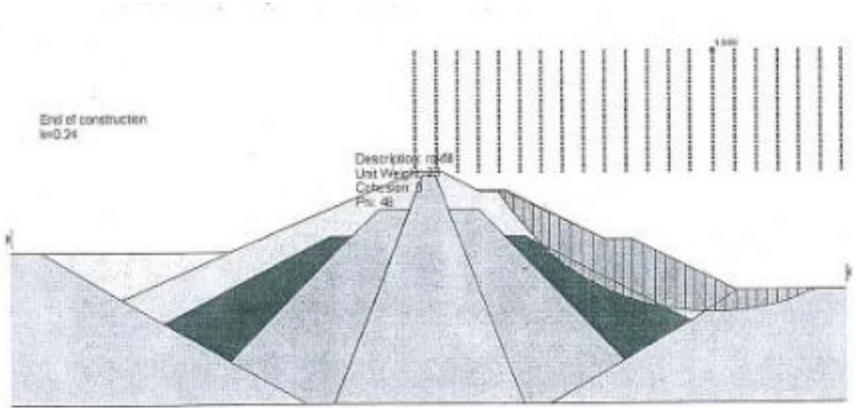

Figure 18. Downstream slope slippage at the end of construction and before operation 699/1=S_f

4.6.3.1.2. Full tank during earthquake (water level at max. W. L)

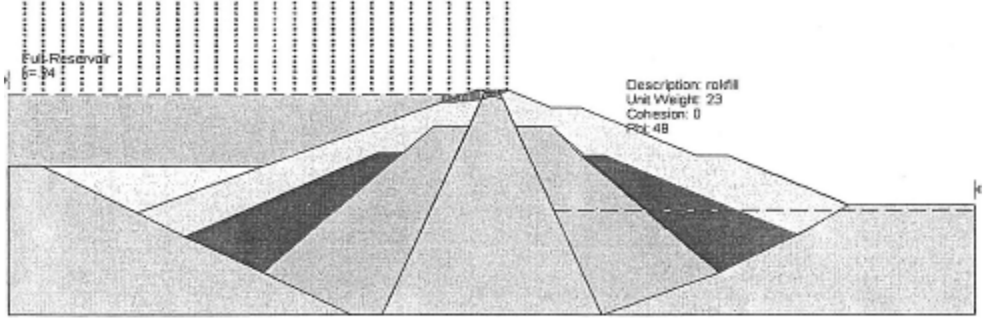

Figure 19. Upstream slope slippage at full tank 687/2=S_f

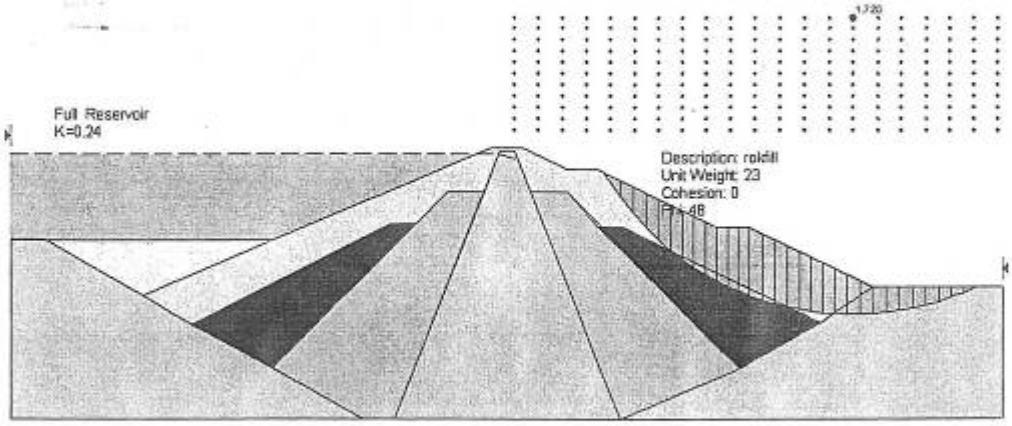

Figure 20. Downstream slope slippage at full tank 72/1=S_f

4.6.3.1.3. rapid depletion

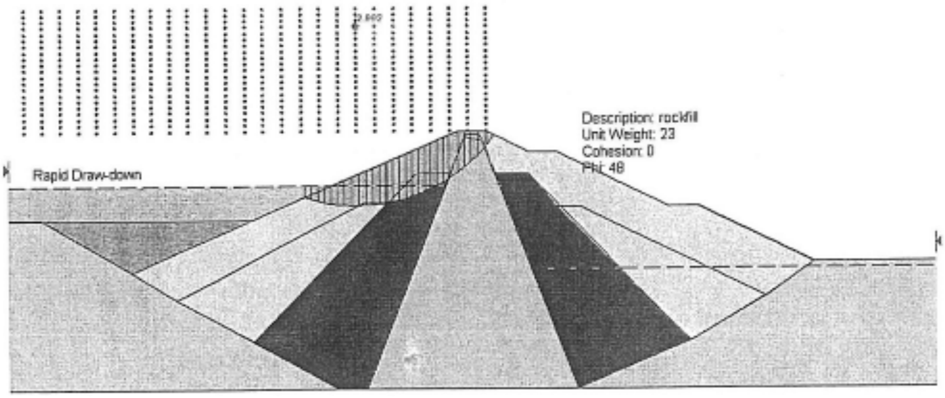

Figure 21. Upstream slope slippage at rapid depletion 992/2=S_f

4.6.3.1.4. half full tank during earthquake

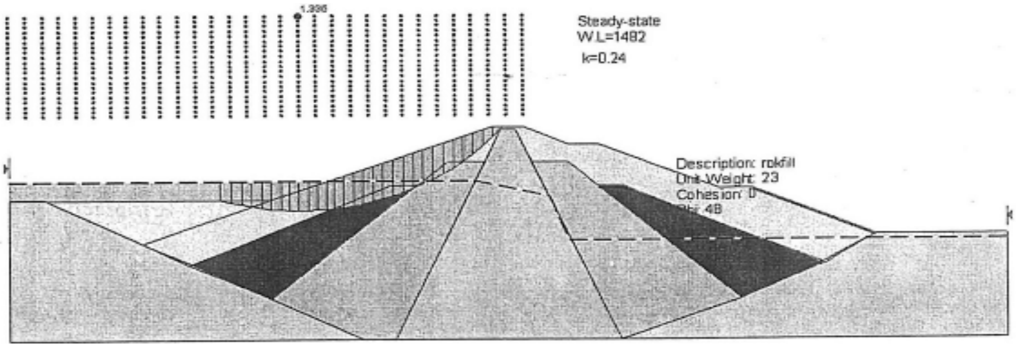

Figure 22. Upstream slope slippage at half full tank 335/1=S_f

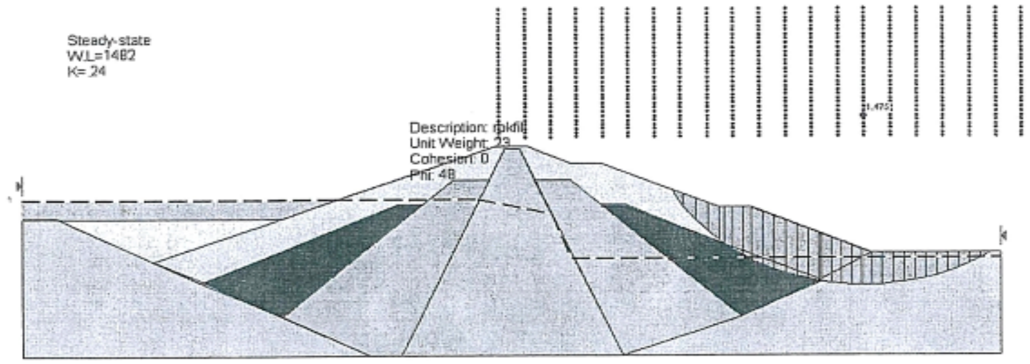

Figure 23. Downstream slope slippage at half full tank 475/1=S_f

According to above mentioned facts, the summary of the results from the stability analysis in Rakfyl $\varphi = 48$ materials mode have been shown in Table 14.

Table 14. Summary of analysis results $\phi = 48$

Analysis conditions	$S_f$upstream	$S_f$downstream
End of construction	1.597	1.692
Full tank	2.687	1.72
Fast discharge	2.992	1.929
Half Full tank	1.335	1.475

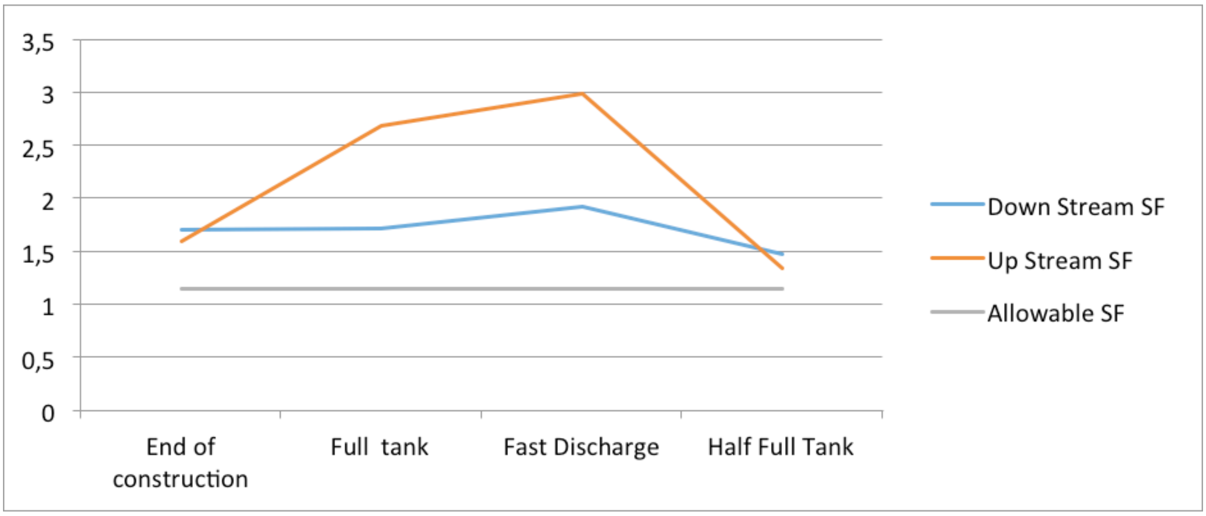

Figure 24. Comparison of the safety factor of the upstream and downstream slopes at an allowed safety factor for different modes studied.

As the results of analysis indicate, in all modes the stability coefficient was obtained to be more than the minimum acceptable value recommended, i.e. 1.15 while in the conditions of half full tank the earthquake ratio of 0.24 was exerted on the structure and the minimum factor of safety was achieved. Since there was a great difference between the safety factor obtained in this critical situation and the acceptable safety recommendations, the low friction materials can be used if necessary as shell materials. The following analyzes were carried out for three different angles and the results are presented in several figures and tables.

4.6.3.2. Results of analyzes in the condition where the shell materials contain $\varphi = 45$

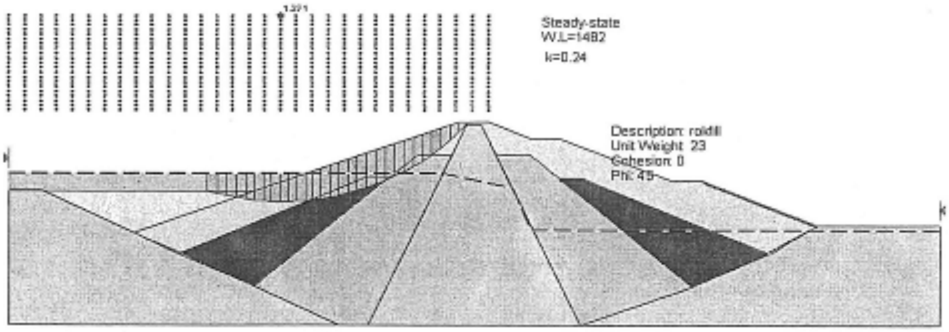

Figure 25. Upstream slope slippage at half full tank 271/1=S_f

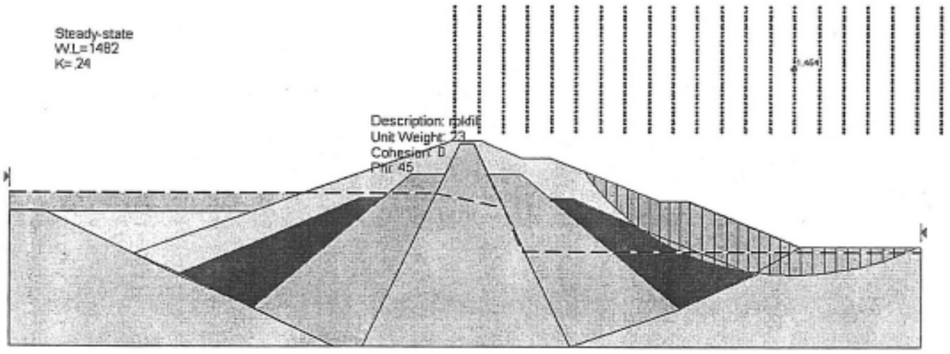

Figure 26. Downstream slope slippage at half full tank 454/1=S_f

4.6.3.3. Results of analyzes in the condition where the shell materials contain $\varphi = 42$

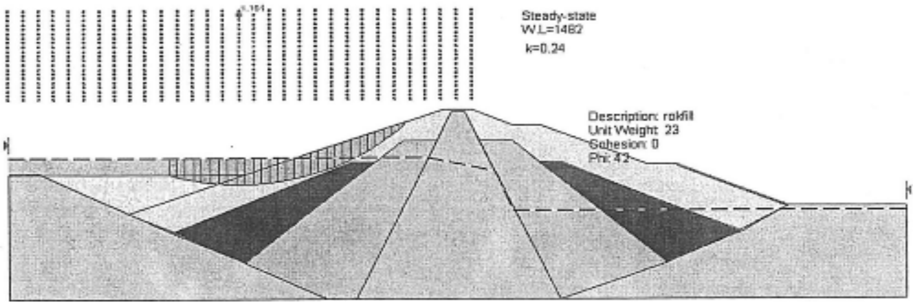

Figure 27. Upstream slope slippage at half full tank 161/1=S_f

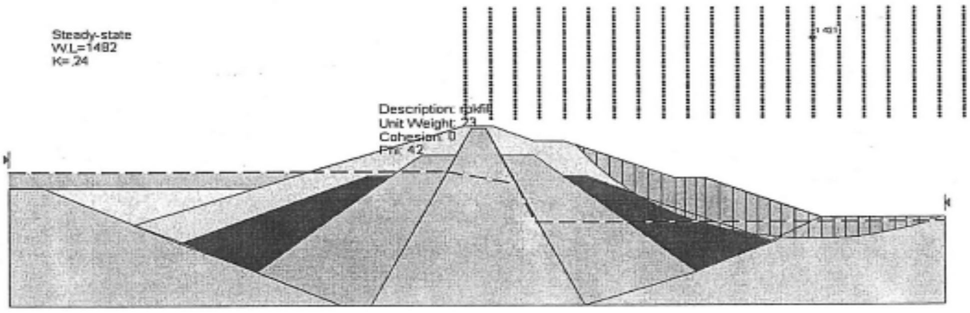

Figure 28. Downstream slope slippage at half full tank 421/1=S_f

According to Figure 4.20, at friction angle of 42 degrees, the safety factor of the upstream angle approaches the boundary conditions. Therefore, the minimum friction angle of the shell material (Rockfill) at upstream slope can be 42 degrees.

4.6.3.4. Results of analyzes in the downstream slope where the shell materials contain $\varphi = 38$

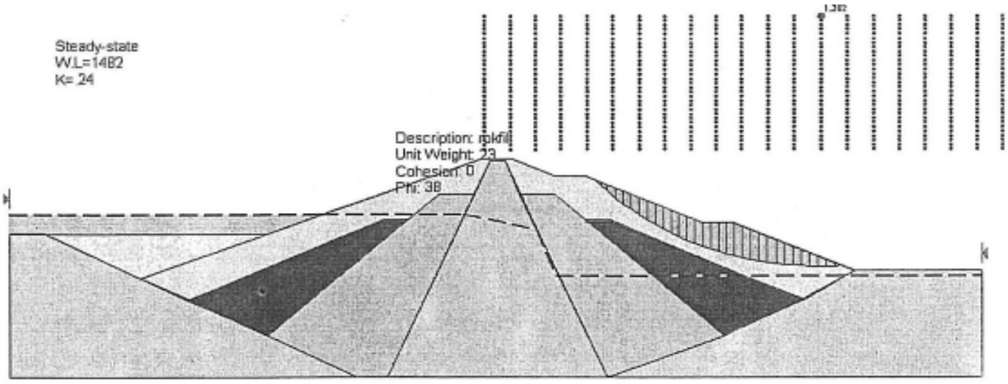

Figure 29. Downstream slope slippage at half full tank 282/1=S_f

4.6.3.5. Results of analyzes in the downstream slope where the shell materials contain $\varphi = 35$

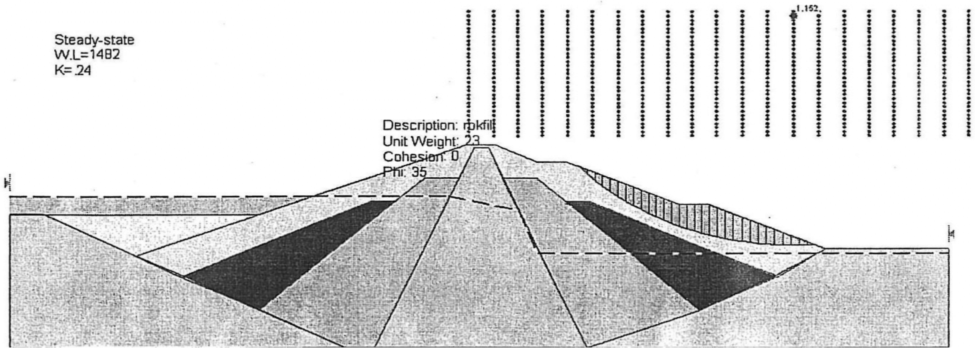

Figure 30. Downstream slope slippage at half full tank 152/1=S_f

Table 15. Summary of the results from the analyzes for the various friction angles of the shell in the most critical condition

Friction angle of the shell	S_f upstream	S_f downstream
48	1.335	1.475
45	1.271	1.454
42	1.161	1.421
38	1.318	1.282
35	1.245	1.152

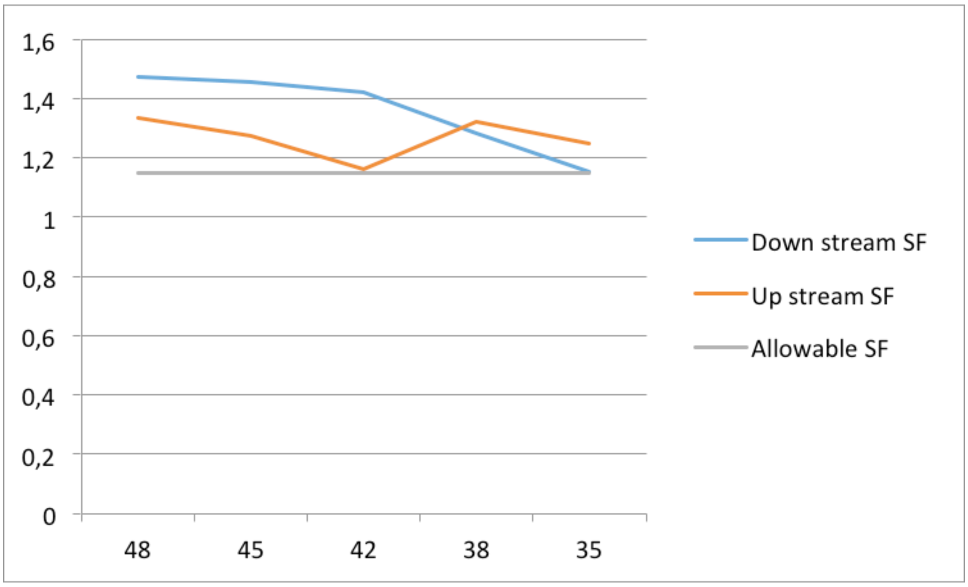

Figure 31. Comparison of allowable safety factor for upstream and downstream slopes for various internal friction angles with rock fill materials

5. CONCLUSIONS

Based on the values obtained from the analysis, the total leakage from the foundation and body of the dam through implementation of one row of waterproof membrane was 44 liters per second, which is equivalent to about 1.4 million cubic meters per year, i.e. the amount of water lost considering the volume exceeds the allowable escape rate of water.

Due to the leakage at allowable rate, it can be concluded that the implementation of the waterproof membrane was to a certain extent successful for controlling the seepage.

Comparing the figures derived from the analysis, it is clear that the amount of leakage in section 21 (left abutment) at the foundation is higher than the right abutment and also the middle section. This seems to indicate that there are areas with incomplete sealing or local pores in the waterproof membrane. As such, these areas act as holes in the membrane creating a conduit for water to escape.

It seems that in the mentioned area (section 21), it is better to implement locally the second row of waterproof membrane.

In order to further secure the structure, it would be better to perform additional drilling boreholes so as to accurately identify and fix up the weak spots of the membrane.

The results indicated that under different conditions, the output gradient is always smaller than 1, which means that the dam is safe against piping.

The clay core was effective in reducing the amount of water leakage. So that leakage of water in the clay core was about 30% less than that of the dam built without clay core.

By analyzing and comparing the results from Slope/W, it can be concluded that the minimum acceptable friction angle for rock fill materials was 42 degrees upstream slope and 35 degrees for downstream slope.

REFERENCES

[1] Ambikaipahan. R., Failure of an Earth Dam. MSc Thesis in Geosciences. Department of Geosciences. Oslo. Norway. 2011.

[2] Berrones, R. F. and Lopez, A. N. Internal Erosion Due to Water Flow Through Earth Dams and Earth Structures. (Publisher Intech, 2011)

[3] Dunbar, S. W; and Sheahan, T.C. Seepage Control Remediation at Hodges Village Dam. Journal of Geotechnical and Geo environmental Engineering, 125 (3), 198-206 (1999).

[4] Ersayin, D. Studying Seepage In A Body Of Earth Fill Dam By Artificial Neural Networks. MSc Thesis . Department of civil Engineering. Izmir Turkey. 2006.

[5] Hassani, H.; Mamizadeh, J.; Karimi, H. Stability of Slope And Seepage Anlayze In Earth-fill Dams Using Numerical Models (Case Study :Ilam Dam- Iran). World Applied Sciences Journal. 21 (9), 1398-1402 (2013).

[6] Hillo, A. Finite Elements For Seepage Below Hydraulic Structure On Anisotropic Soil Foundation. MSc Thesis. College of Engineering. University Of Basreh. Iraq. 2007.

[7] Hosseini, S. M; Fard, R. A. Pore Pressure Development in the Core of the Earth Dams During Simultaneous Construction and Impounding. Journal of EJGE. http:// www.ejge.com (2002)

[8] Irzooki, R. H. Investigation And Analysis of Seepage Problems on The Left Side of Al-Quadisia Dam. PH.D Thesis. Department of Building and Construction Engineering. University of Technology. Iraq. 1998.

[9] Kiyani, M. Determining The Optimum Depth for Sealing in Earth-fill Dams (Case study: Gotvand Dam- Iran). M.Sc Thesis . Department of Civil Engineering. Tabriz University. 2011.

[10] Khsaf, S.I. Numerical Analaysis of Seepage problems with Flow Control Devices Underneath Hydraulic Structures. PH.D Thesis. Dept of Building and Construction Engineering. College of Eengineering. University of Technolgy. Iraq. 1998.

[11] Naseh, S.; Ghafoori, M.; Hafezi Moghaddas ,N.; Lashkaripur, G. Investigation of Seepage Paths in Left Abutment of Bidvaz Dam Using Tracing Technique. International Journal of Emerging Technology and Advanced Engineering. 3 (4), 719-724 (2013)

[12] Robertson, P. K. Evaluation of Flow Liquefaction and Liquefied Strength Using The Cone Penetration Test. Journal of Geotechnical and Geo environmental Engineering. 136 (6), 842-853 (2010)

[13] Tayfur, G.S.; Wita, A.; Singh, V. Case Study Finite Element Method and Artificial Neural Network for Flow through Jeiziorsko Earth-fill Dam in Poland. J.Hydrual.Eng. 136 (1), 431-440 (2005).

[14] Yilmaz, I. Ersin ,Y. Selection of Core material for an Earth Dam in The Lower Cekerek Basin, Tokat, Turkey. Journal Of EJGE. http:// www.ejge.com/2004/ppr0472/abs0472 (2004).

[15] Yusif al Labban, S.N. Seepage Analysis of Earth Dam by Finite Element. MS.c Thesis. College of Engineering University of Kufa. Iraq. 2007